



Identification of Germline Non-coding Deletions in XIAP Gene Causing XIAP Deficiency Reveals a Key Promoter Sequence

Zineb Sbihi, Kay Tanita, Camille Bachelet, Christine Bole, Fabienne Jabot-Hanin, Frederic Tores, Marc Le Loch, Radi Khodr, Akihiro Hoshino, Christelle Lenoir, et al.

► To cite this version:

Zineb Sbihi, Kay Tanita, Camille Bachelet, Christine Bole, Fabienne Jabot-Hanin, et al.. Identification of Germline Non-coding Deletions in XIAP Gene Causing XIAP Deficiency Reveals a Key Promoter Sequence. *Journal of Clinical Immunology*, 2022, 42 (3), pp.559-571. <10.1007/s10875-021-01188-z>. <hal-03864194>

HAL Id: hal-03864194

<https://hal.science/hal-03864194v1>

Submitted on 23 Nov 2022

HAL is a multi-disciplinary open access archive for the deposit and dissemination of scientific research documents, whether they are published or not. The documents may come from teaching and research institutions in France or abroad, or from public or private research centers.

L'archive ouverte pluridisciplinaire **HAL**, est destinée au dépôt et à la diffusion de documents scientifiques de niveau recherche, publiés ou non, émanant des établissements d'enseignement et de recherche français ou étrangers, des laboratoires publics ou privés.



HAL Authorization

Identification of germline non-coding deletions in XIAP gene causing XIAP deficiency reveals a key promoter sequence

Zineb Sbihi¹, Kay Tanita², Camille Bachelet^{1,3}, Christine Bole⁴, Fabienne Jabot-Hanin^{4,5}, Frederic Tores^{4,5}, Marc Le Loch⁶, Radi Khodr¹, Akihiro Hoshino¹, Christelle Lenoir¹, Matias Oleastro⁷, Mariana Villa⁷, Lucia Spossito⁷, Emma Prieto⁷, Silvia Danielian⁷, Erika Brunet⁸, Capucine Picard^{1,3,9}, Takashi Taga¹⁰, Shimaa Said Mohamed Ali Abdrabou¹¹, Takeshi Isoda², Masafumi Yamada¹¹, Alejandro Palma⁷, Hiro Kanegane¹² and Sylvain Latour^{1,3}

¹Laboratory of Lymphocyte Activation and Susceptibility to EBV infection, INSERM UMR 1163, Imagine Institute, Paris, France;

²Department of Pediatrics and Developmental Biology, Graduate School of Medical and Dental Sciences, Tokyo Medical and Dental University (TMDU), Tokyo, Japan;

³Université de Paris, Paris, France;

⁴Genomics Core Facility, Institut Imagine-Structure Fédérative de Recherche Necker, INSERM U1163 et INSERM US24/CNRS UMS3633, Université de Paris, Paris, France;

⁵Bioinformatic Platform, INSERM UMR 1163, Institut Imagine, Paris, France;

⁶Service d'Histologie - Embryologie - Cytogénétique, Hôpital Necker-Enfants Malades, Paris, France;

⁷Immunology and Rheumatology Division, Hospital de Pediatria S.A.M.I.C. Prof. Dr. Juan P. Garrahan, Buenos Aires, Argentina;

⁸Laboratory of Dynamic of Genome and Immune System, INSERM UMR 1163, Imagine Institute, Paris, France;

⁹Study Center for Primary Immunodeficiencies, Necker-Enfants Malades Hospital, APHP, Paris, France;

¹⁰Department of Pediatrics, Shiga University of Medical Science, Otsu, Japan;

¹¹Department of Pediatrics, Faculty of Medicine, Graduate School of Medicine, Hokkaido University, Sapporo, Japan;

¹²Department of Child Health and Development, Graduate School of Medical and Dental Sciences, TMDU, Tokyo, Japan.

Contact information:

Corresponding author: Dr Sylvain Latour, E-mail: sylvain.latour@inserm.fr ; Tel: +33 (1) 42 75 43 03; Fax: +33 (1) 42 75 42 21.

Key words: X-linked inhibitor of apoptosis ; inherited immunodeficiency ; non-coding exon ; deletion ; promoter

Abstract

Purpose: X-linked inhibitor of apoptosis protein (XIAP) deficiency, also known as the X-linked lymphoproliferative syndrome of type 2 (XLP-2), is a rare immunodeficiency characterized by recurrent hemophagocytic lymphohistiocytosis, splenomegaly and inflammatory bowel disease. Variants in XIAP including missense, non-sense, frameshift and deletions of coding exons have been reported to cause XIAP deficiency. We studied three young boys with immunodeficiency displaying XLP-2-like clinical features. No genetic variation in the coding exons of XIAP was identified by whole exome sequencing (WES), although the patients exhibited a complete loss of XIAP expression.

Methods: Targeted next-generation sequencing (NGS) of the entire locus of XIAP was performed on DNA samples from the three patients. Molecular investigations were assessed by gene reporter expression assays in HEK cells and CRISPR-Cas9 genome editing in primary T cells.

Results: NGS of XIAP identified three distinct non-coding deletions in the patients that were predicted to be driven by repetitive DNA sequences. These deletions share a common region of 839bp that encompassed the first non-coding exon of XIAP and contained regulatory elements and marks specific of an active promoter. Moreover, we showed that among the 839bp, the exon was transcriptionally active. Finally, deletion of the exon by CRISPR-Cas9 in primary cells reduced XIAP protein expression.

Conclusions: These results identify a key promoter sequence contained in the first non-coding exon of XIAP. Importantly, this study highlights that sequencing of the non-coding exons that are not currently captured by WES should be considered in the genetic diagnosis when no variation is found in coding exons.

Introduction

X-linked inhibitor of apoptosis (XIAP) deficiency (OMIM #300635), also known as the X-linked lymphoproliferative syndrome type 2 (XLP-2), is a recessive inherited primary immunodeficiency estimated to affect approximately 1-3 males per million, although it may be underdiagnosed. XIAP deficiency is associated with a high risk to develop inflammatory symptoms including hemophagocytic lymphohistiocytosis (HLH) often in response to EBV infection, recurrent splenomegaly, inflammatory bowel disease (IBD) with the features of Crohn's disease [1-6]. Notably, heterozygous females can also develop symptoms as severe as in males due to abnormal X-inactivation [4, 7].

XIAP was originally described as an anti-apoptotic molecule ubiquitously expressed. It is composed of three Baculovirus inhibitor of apoptosis protein repeat (BIR) domains, a ubiquitin binding domain (UBA), and a C-terminal RING domain with E3 ubiquitin ligase activity. XIAP inhibits programmed cell death by binding to and blocking activated forms of the effector caspases 3, 7 and 9 [8]. In addition to its anti-apoptotic function, XIAP is also involved in several other pathways, including regulation and activation of innate immunity and inflammation [9]. In particular, XIAP is required for signaling and activation of the nucleotide oligomerization domain (NOD) receptors NOD1 and NOD2, which are intracellular sensors of bacterial products [10, 11]. XIAP-deficient monocytes from patients display an impaired production of cytokines and chemokines in response to stimulation with NOD2 ligands, while XIAP-deficient T cells exhibit increased apoptosis when activated [1, 12, 13].

Mutations in XIAP gene have been reported in more than 100 patients worldwide since 2006 [1]. All the mutations described to date are in the coding exons and non-coding flanking regions of exons of *XIAP*. Those include missense mutations and nonsense mutations (n=57), mutations of canonical splice site (n=7), small insertions (n=10), small deletions (n=25), large

84 insertions/duplications (n=3) and deletions (n=15) (Web resources, The human Gene Mutation
85 Database, HGMD 2020.4) (**Figure S1**) [5-7, 11, 13-17].

86 To date, the contribution of disrupted potentially *cis*-regulatory conserved non-coding
87 sequences (CNCs) to human genetic diseases is largely underestimated, as no systematic screen
88 for putative deleterious variations in CNCs has been conducted. Several variants in non-coding
89 gene promoter and regulatory elements regions have been identified in genetic diseases. The
90 majority of them mediates their regulatory effects through alteration of transcriptional factors
91 binding and disturb trans-activation of the target gene promoter [18-21]. Promoter mutations
92 have also been identified in cancer predisposition genes, like in the alternative promoter of *APC*
93 that disrupts the binding of YY1 and reduces APC 1B promoter activity in human gastric cell
94 lines [22]. In familial melanoma, mutations in the TERT promoter altered the binding to
95 transcriptional factors leading to increased TERT promoter activity in human melanoma cell
96 lines [23]. Most recently, whole genome sequencing of a cohort of patients with sporadic
97 immunodeficiency identified compound heterozygosity of coding variants associated with non-
98 coding *cis*-regulatory element (CRE) deletions in *LRBA*, *DOCK8* and *ARPC1* genes,
99 demonstrating that sequence variations within non-coding regions of the genome have effects
100 on gene expression and can contribute to primary immunodeficiency [20]. Furthermore, recent
101 studies have provided insights into the biological relevance of the non-protein-coding portions
102 of the human genome [24]. One of them, the ENCODE pilot study revealed that functional
103 genomic elements are in much higher numbers than previously anticipated, and that the
104 majority of elements regulating gene expression are contained in the non-protein coding regions
105 [25].

106 In the present study, we report the identification of patients with XIAP deficiency whom
107 did not carry mutations in coding regions of *XIAP*, but distant deletions in non-protein coding

108 regions encompassing the non-coding exon 1 of *XIAP* that defines a key promoter sequence
109 required for XIAP expression.

Methods

Exome sequencing and analysis. Genomic DNA from whole blood or peripheral blood cells of patients, their parents, and other family members was isolated according to standard methods. Exome capture and analysis were performed as previously described [26].

Targeted resequencing by NGS. A custom capture by hybridization approach and method were used as previously described [27-30]. The biotinylated single strand DNA probes targeting all the region of interest were designed to cover a 143-kb chromosomal region including the *XIAP* gene on chromosome X: 122904611-123047997 genomic position according to the GRCh37/hg19 assembly of the human reference genome. The capture by hybridization libraries were sequenced using a paired-end mode 100+100 bases on an Illumina NovaSeq6000, to produce ~40 millions of clusters per sample. After demultiplexing, sequences were aligned to the reference human genome hg19 using the Burrows-Wheeler Aligner [31]. The mean depth of coverage per sample was ~200X. Downstream processing was carried out with the Genome Analysis Toolkit (GATK), SAMtools and Picard, following documented best practices (<http://www.broadinstitute.org/gatk/guide/topic?name=best-practices>). Variant calls were made with the GATK Unified Genotyper. The annotation process is based on the latest release of the Ensembl database. Variants were annotated and analyzed and prioritized using the Polyweb/PolyDiag software interface designed by the Bioinformatics platform of University Paris Descartes (Polyweb Imagine, <https://www.polyweb.fr>). Sequences were aligned with the hg19 reference human genome with Burrows-Wheeler Aligner, version 0.6.2.13. CNVs were analyzed using Integrative Genome Viewer (IGV) software (<https://software.broadinstitute.org/software/igv/> or <https://igv.org>).

Apoptosis assays. 2×10^5 T-cell blasts/well were seeded into 96-well plates pre-coated with 0.1, 1 or 10 $\mu\text{g/ml}$ of mAb anti-CD3 OKT3 (eBioscience), or incubated with anti-CD3/CD28-coated beads (Invitrogen). Apoptotic cells were detected after overnight stimulation by

propidium iodide staining according to standard protocol [1]. Cells were washed with PBS twice, and data were acquired using a LSRFortessa (BD Biosciences) and analyzed using FlowJo X (TreeStar). The percentage of induced apoptosis was calculated according to the formula: $100 \times (\% \text{ of experimental apoptotic cells} - \% \text{ of spontaneously apoptotic cells} / 100 - \% \text{ of spontaneously apoptotic cells})$.

Analysis of protein expression by immunoblotting. Protein extracts from PBMC and T-cell blasts were obtained and analyzed as previously described [1, 26]. Proteins were separated by SDS-PAGE and transferred on PVDF membranes (Millipore). Membranes were blocked with milk for 1 hour before incubation with primary antibodies. The following antibodies were used for immunoblotting: anti-XIAP (clone hILP, BD Bioscience), anti-KU80 (clone C48E7, Cell Signaling) and anti-ACTIN (clone 13E5, Sigma-Aldrich). Membranes were then washed and incubated with anti-mouse or anti-rabbit HRP-conjugated antibodies (Cell Signaling). Pierce ECL western blotting substrate was used for detection (ThermoFisher). Densitometry analyses were performed using ImageJ software and normalized to loading western blot KU80 controls.

In Silico analysis. To identify potential regulatory elements within the *XIAP* deletion region, we used DNaseI sequencing data along with histone modification ChIP-seq data from ENCODE (Encyclopedia of DNA elements) [32]. Bioinformatics analyses on deleted regions were performed using publically available datasets from ENCODE, which includes information such as the location of promoter and enhancer histone marks, open chromatin and bound proteins.

Luciferase Assay. Primers were designed to amplify a genomic region that encompasses potential XIAP regulatory regions. A 892bp product (chrX: 122993332–122994223) corresponding to the commonly deleted region of *XIAP* sequence containing upstream sequence, non-coding exon1, and partial intron 1 of the *XIAP* gene, or a 417bp product (chrX: 122993756–122994173) containing non-coding exon1, and partial intron1, or A 359bp product

160 (chrX: 122993421–122993779) containing upstream sequence of the *XIAP* gene, were
161 amplified from control genomic DNA, cloned into the promoter-less firefly luciferase reporter
162 vector pGL3-Basic (Promega). Primers used for cloning incorporated KpnI and XhoI restriction
163 site to facilitate subcloning are listed in **Table S1**. All the constructs were verified by Sanger
164 sequencing (Applied Biosystems). pGL3-Basic plasmids containing the promoter sequences of
165 *XIAP* (90ng) were co-transfected with 10 ng of pRL-CMV (CMV-promoter driven *Renilla*
166 luciferase reporter, Promega) in HEK293 cells using lipofectamine 2000 (Invitrogen) according
167 to the manufacturer's instructions. 24h post-transfection, luciferase activity was measured using
168 a dual-luciferase reporter assay system according to the manufacturer's instructions (dual-Glo
169 Luciferase reporter assay, Promega).

170 ***Cas9 RNP-mediated Editing of primary human T cells.*** T-cell blasts were activated with anti-
171 CD3/CD28-coated beads (Invitrogen) for 48 hours prior to electroporation with
172 ribonucleoprotein/RNP complexes using the P3 Primary cell 4D X kit and 4D-Nucleofector
173 (Lonza). The *Streptococcus pyogenes* Cas9 protein with 2 nuclear localization signals (NLS)
174 expressed and purified as described by Menoret et al. [33], was kindly provided by Dr. J.P.
175 Concordet (Structure and Instability of Genomes laboratory, Muséum National d'Histoire
176 Naturelle, France). The following *XIAP* gene-specific sgRNAs, designed using the online tool:
177 <http://crispor.tefor.net> [34], were used: sgRNA1: 5'-CUGGGAUAGUUAUCCCCUGU-3' ;
178 sgRNA2: 5'-UUCCUCGGACUGCCGACGGC-3' ; sgRNA3: 5'-
179 CCAGCCCGGGCUGCGCCACU-3'; sgRNA4: 5'-GCGGUGGGUACAGCUUGUGU-3'.
180 Chemically modified sgRNAs were purchased from Synthego with protospacer adjacent motif
181 (<https://www.synthego.com>). To generate Cas9 RNP complexes, *Streptococcus pyogenes* Cas9
182 protein (90µM) and sgRNAs (180µM) were mixed 1 : 2. For each condition, 4.10⁶ stimulated
183 T-cell blasts were transfected with the Cas9 RNP mix using program CA-137 on the Amaxa
184 4D-Nucleofector (Lonza). 300µL pre-warmed complete medium was added to each well, and

185 the cells were allowed to recover for 10 min at room temperature. Cells were then plated in 1
186 mL of medium with 100IU of IL2, and maintained at 1.10^6 cells / mL for 20 days. The region
187 on genomic DNA that spans the cutting site of each sgRNA (sgRNA1, sgRNA2, sgRNA3, and
188 sgRNA4) was amplified by PCR using the following on-target primers: forward: 5'-
189 CTTTGTTTCCGGTCCATCTGC-3' and reverse: 5'-CGGAAGCTCTTTGGCCCTTA-3';
190 forward: 5'-AAGAAACACTGGAGCTGGGG-3' and reverse: 5'-
191 AATCCTGCAGGCCTGAAGTC-3', respectively (Eurofin). Amplified products were
192 separated by agarose gel electrophoresis and Sanger sequenced (Applied-Biosystems).

Results

Identification of three unrelated patients presenting XIAP deficiency-like features

We investigated three male patients with immunodeficiency from three unrelated families one from Argentina (Patient 1, P1), and two from Japan (Patient 2, P2 and Patient 3, P3) (**Figure 1A**). P1 became symptomatic within the first months of life, P2 by the age of 18 months, and P3 by the age of 9 years. All patients presented with recurrent **severe** HLH triggered (P1) or not (P2 and P3) by EBV infection; this was the first clinical manifestation in the three patients (**Table 1**). In P1 and P2, HLH was associated with persistent splenomegaly associated with fluctuating thrombocytopenia in P1 and pancytopenia in P2. P1 was treated by cyclosporine and prednisone. P2 was treated by dexamethasone and was refractory to intravenous immunoglobulin. P3 developed inflammatory bowel disease (IBD) concomitantly to HLH and was refractory to treatments with steroid, infliximab and tacrolimus. He underwent several colectomies between 9 and 18 years old, and finally received allogeneic hematopoietic stem cell transplantation at 19 years of age and he is well since (**Table 1**).

Absence of XIAP expression in cells of patients

Because HLH, IBD and splenomegaly are clinical features reported to be associated with XIAP deficiency [35], XIAP deficiency was evaluated as a possible cause of the clinical symptoms in the three patients. XIAP expression was first examined in PBMCs from P1 and P2 by intracellular staining by flow cytometry suggesting a reduced XIAP expression (**Figure S2A and data not shown**). However, we experienced that this method frequently led to false positive as exemplified by a patient with a deletion in the coding exon 3 of XIAP with apparent normal XIAP expression by flow cytometry, while there was no XIAP expression by western blot (**Figure S3 and data not shown**). Thus, XIAP expression was assessed by western blot in cell extracts of T lymphocytes from P1, P2 and P3. No detectable expression was observed in cells of P1, P2 and P3, in contrast to the reliable XIAP expression detected in lysates of control

T cells from healthy donors (**Figure 1B and data not shown for P3**). Moreover, analysis of *XIAP* transcripts by PCR in cells of patients P1, P2 and P3 failed to amplify *XIAP* transcripts in comparison to the control cells in which *XIAP* transcripts were detected (**Figure 1C and data not shown for P3**). Increased activation-induced cell-death of T lymphocytes and defective NOD2-mediated IL-8 production by myeloid cells, which represent two major hallmarks of the *XIAP* deficiency [1, 4], were observed respectively in T cells of patient P1 and in PBMCs of P2 and P3 (**Figure S2B and C**). Therefore, these data strongly suggested that the three patients had a *XIAP* deficiency explaining their clinical phenotypes.

Identification of large deletions in 5' non-coding regions of *XIAP* in three patients

We thus investigated the *XIAP* gene in the three patients for genetic variations that could explain their loss of *XIAP* expression. Surprisingly, whole-exome sequencing (WES) performed in P1 failed to identify genetic variations in *XIAP*, although the sequencing coverage of the six coding exons of *XIAP* was significant (**data not shown**). In patients P2 and P3, targeted Sanger sequencing of the 6 coding exons including non-coding flanking regions (of 50-80bp) was conducted and did not reveal any genetic variations (**data not shown**). Therefore, in P1, P2 and P3, the *XIAP* deficiency was not caused by mutations in 6 coding exons of *XIAP*, suggesting another mechanism(s), since all mutations in *XIAP* reported so far to cause *XIAP* deficiency target the 6 coding exons (**Figure 1S**).

Given that variants within a non-coding or regulatory region are missed by WES or by targeted sequencing, we next performed high-throughput targeted resequencing with custom capture oligonucleotides designed to cover a large region of 87386bp encompassing the *XIAP* locus (from g.122960611 to g.123047997) (**Figure 2**). This region includes 80 kb of sequences 5' to the start codon and 7 kb of the sequences 3' to the stop codon. Patients and their parents (when available) as well as two healthy controls were analyzed. We searched for rare single-nucleotide variants (SNVs), insertions and deletions (indels). Confirming the first analyses, no

SNVs or indels in the 6 coding exons were detected in the three patients. However, there was no sequence reads in regions between the 5' region and the first intron 1 encompassing the non-coding exon1 in P1, P2 and P3, indicating hemizygous deletions in the 5' region of *XIAP* in the three patients. In P2, one short deletion and one long deletion were detected. The coverage (or numbers of reads) of this region in the mother of P1 was twice that in the father and in a healthy male control, suggesting that the hemizygous deletion in P1 was *de novo* or transmitted through germline mosaicism. The coverage of the long deletion in the mother of P2 was equivalent to a healthy male control and reduced about twice compared to a healthy female control and around 50% of reads carried the same deleted region as in P2, suggesting that the hemizygous long deletion in P2 was inherited from the mother (**Figure 2** and **Figure S4**). Similarly, the short deletion in P2 was also inherited from the mother, but was found to be homozygous in the mother as no wild-type reads were detected (**Figure S4**). In family 3, the mother of P3 was not analyzed by NGS, but the deleted region was successfully amplified by PCR from DNA of the mother strongly supporting mother inheritance of the deletion (**Figure S4C**).

To confirm these findings and precisely map the limits of these deletions, targeted amplification by PCR and Sanger sequencing of surrounding regions of deletions were performed. In P1 and P3, amplicons were obtained and sequenced, demonstrating hemizygous deletions of 21,521bp (chrX: g.122979032_123000553del, hereafter denoted as $\Delta 1$) and 2,199bp (chrX: g.122993375_122995574del, hereafter denoted as $\Delta 3$), respectively (**Figure 3A and B** and **Figure S4**). PCR products were amplified in mother of P3, but not in mother of P1 confirming the maternal transmission in P3 and the *de novo* or maternal transmission through germline mosaicism in P1 (**Figure S4**). In P2, we failed to amplify the regions surrounding the two deletions in P2 possibly due of the GC enrichment. Hence, the limits of the deletions in P2 were only assessed by analysis of NGS data showing two hemizygous deletions of 862bp and 17,979bp (chrX: g.122972822_122973684del and

g.122976235_122994214del, hereafter denoted $\Delta 2a$ and $\Delta 2b$) (**Figure S5 and Figure 3A and 3B**). Therefore, these data identified deletions in 5' non-coding regions in *XIAP* in the three patients that likely account for their *XIAP* deficiency.

Analysis of repeat elements at the *XIAP* locus and mechanisms underlying the three deletions

Double strand breaks (DSBs) when occurring in repeated elements are associated with genome instability including deletions. DSB repair by homologous recombination or by a non-homologous end-joining repair mechanism may lead to crossovers between two repeated sequences or micro-homologies in sequences resulting in the excision of the intervening region [36, 37]. Thus, we next investigated whether the breakpoint regions of the three deletions were located within repeated elements (**Figure 3A**). First, using RepeatMasker program (see Web resources), we determined the percentage of repeated elements including *Alu* elements, *Line* elements, DNA transposons and C-rich elements in the *XIAP* locus. We found that 64.58% of the *XIAP* locus consists of repeated elements including 42.97% of *Alu* elements, 18.17% of long Interspersed Nuclear (*LINEs*) elements and 1.9% of simple sequence repeats. Repeated elements represent 62% of the genome of the X chromosome and among them 10% are *Alu* elements (from Bioinfo-fr, Human genome repeated elements, see Web resources). The *XIAP* locus can thus be considered to be enriched in repeated elements in particular *Alu* elements. As expected these repeated elements are preferentially located in the non-coding regions of the *XIAP* locus: the 5' region, 3' region, and intronic regions (**Figure 3A**). Alignments of the breakpoints with UCSC Genome Browser data [38] showed that the four deletions were located within 4 different repeat elements: *AluSx* in the 5' region and *AluSx4* in intron1-2 for $\Delta 1$; *AluSq2* in the 5' region and *AluSx1* elements in intron 1-2 for $\Delta 2a$; *AluSp* in the 5' region and *C-rich* elements in intron 1-2 for $\Delta 2b$; and one *MIR* in the 5' region and low complexity repeats consisting of DNA transposons n(TA) in intron 1-2 for $\Delta 3$ (**Figure 3B and Table S2**).

Junctional micro-homologies observed at the breakpoints suggested that deletions were formed by DSBs repair mechanisms such as replicative based-repair, non-homologous end-joining/NHEJ and/or alternative end-joining (also termed microhomology mediated end-joining/MMEJ) mechanisms [36]. Another possible mechanism is the non-allelic homologous recombination that could occur between repetitive elements of the same family such in $\Delta 1$ and $\Delta 2a$. Microhomology of 1-4bp rather facilitate NHEJ that may account for $\Delta 1$ and $\Delta 3$, while microhomology up to 5bp as found in $\Delta 2a$ and $\Delta 2b$ may favor a MMEJ-dependent mechanism. The deletion of one nucleotide (C) in $\Delta 3$ at the breakpoints strongly supports a NHEJ or MMEJ-dependent repair mechanism at work, as both are prone to errors and could lead to base excision. However, these observations indicated that the three deletions are located in repeated sequences prone to genomic rearrangements.

The first non-coding exon in *XIAP* deleted in the three patients hold characteristics of a promoter sequence

Importantly, intersection of the three deletions revealed a commonly deleted region of 839bp in the three patients (g.122993375_122994214del). This deleted region contains 5' UTR sequences and the first non-coding exon1 of *XIAP* of 267 pb (chrX: g.122993877_122994143) (**Figures 2 and 4 and Figure S4**). Using ENCODE databases, we analyzed this region to determine whether it contains regulatory and/or promoter elements (**Figure 4A and Figure S6**). The 839bp region was predicted to be enriched in regulatory promoter elements corresponding to a putative promoter (between chrX: g.122992320 and 122996142 corresponding the red box in Figure 3A), **Figure 4A**). Notably, interrogation of chromatin immunoprecipitation sequencing (ChIP-seq) ENCODE data revealed that this region is transcriptionally active with multiple binding sites for different transcription factors (**Figure 4A and Table S3**). Moreover, this region was found within an accessible and active chromatin region as determined by ENCODE derived DNase I hypersensitive clusters and enrichment for

promoter histone modifications (H3K4me3) and active histone modifications (H3K27ac). These observations strongly suggested that this region has a promoter activity and, thus its deletion accounts for the XIAP deficiency in the patients.

The first non-coding exon in *XIAP* contains active promoter sequences required for XIAP expression

To further characterize the role of the non-coding exon1 as a promoter sequence, the 839bp region was divided in two, one containing 3'sequences corresponding to exon1 and one corresponding to 5'sequences flanking exon1 (**Figure 4B**). The entire 839bp and the two sub-regions were cloned in a gene expression reporter vector at the 5' of the ATG of the luciferase gene. The vectors were transiently transfected in HEK cells and luciferase activity was measured (**Figure 4C**). Luciferase activity was significantly detectable in cell-extracts of cells transfected with the entire 839bp region or the 3'sequences containing exon1, but not in extracts from cells transfected with the 5'sequences flanking exon1. As a positive control of luciferase activity, cells were transfected with a vector coding the transcription factor EOMES in combination with the reporter gene vector, in which the luciferase was under the control of the proximal *IFNG* promoter that is known to be activated by EOMES. Therefore, these data indicate that the 839bp region has a promoter activity that is contained in sequences containing the non-coding exon1.

To formally demonstrate that the non-coding exon1 of *XIAP* contained a key promoter sequence required for XIAP expression, we used CRISPR/Cas9 gene editing to obtain primary T cells from healthy control males in which the non-coding exon1 was deleted (**Figure 5**). We designed two pairs of single-guide RNAs (sgRNAs), one pair targeting a locus containing the 839bp region commonly deleted in the three patients, sgRNA1 and sgRNA2, while the second targeted a locus restricted to *XIAP* non-coding exon1. Cleavages by sgRNA1 and sgRNA2 or by sgRNA3 and sgRNA4 theoretically resulted respectively in a 1050bp deletion

(XIAP Δ 1050bp, containing the 839bp region) and in a 300bp deletion (XIAP Δ 300bp, containing the exon1) (**Figure 5A**). XIAP-targeting sgRNA guides complexed with the Cas9 protein were delivered to activated T cell blasts, and cells were further expanded for genetic, molecular and functional validation of the gene editing. Two regions of 1456bp and 843bp encompassing the 1050bp and 300bp deletions respectively were amplified from DNA extracted from cells following expansion at day 5 and day 13 after Cas9-sgRNAs delivery. Only PCR products from cells that received Cas9 complexed with both sgRNA1 and sgRNA2 or both sgRNA3 and sgRNA4 showed specific deletions of 1050bp and 300bp respectively (**Figure 5B**). However, wild-type sequences were still present indicating that only a fraction of cells has been targeted. Since we used pairs of sgRNAs to create deletions, we could not evaluate the % of edited cells using TIDE or ICE tools. However, based on the intensities of the PCR products in the gel, we estimated that roughly 30-40% of cells carried the 1050bp deletion and around 50% of cells had the 300pb deletion. In contrast, no specific deletion was observed with Cas9-RNPs containing single sgRNA, scramble sgRNA or no sgRNA. The deletions were confirmed by Sanger sequencing of the PCR products (**Figure 5C**). Immunoblotting of lysates from cells having received Cas9-RNPs containing both sgRNA1 and sgRNA2 or both sgRNA3 and sgRNA4 showed a significant reduction of XIAP expression relative to non-targeting controls (**Figure 5D**). The expression of XIAP was not completely abolished likely because only a fraction of cells was targeted as indicated by the PCR analyses (**Figure 5B**). Finally, this reduction in XIAP expression was associated with an increase of activation-induced cell death/apoptosis in T cells stimulated with anti-CD3 antibody (**Figure 5E**). Taken together, these data demonstrated that the non-coding exon1 contains key promoter sequences required for XIAP protein expression.

Discussion

The genetic basis of diseases is mainly focused on coding regions. However, more and more evidence is coming now, that a large proportion of non-coding sequences in the genome is functional and harbors genetic variants which contribute to disease etiology. In this study, we reported three XIAP-deficient young male patients from three unrelated kindreds originating from Japan and Argentina. The three patients studied have XLP-2-like clinical features, associated with typical manifestation with HLH, IBD and splenomegaly. Surprisingly, no genetic variation in the coding exons of XIAP was identified by whole exome sequencing (WES), although the patients exhibited a complete loss of XIAP expression. We reported here first XIAP-deficiency associated with a large non-coding hemizygous deletions. The deletions reported here lead to a complete absence of XIAP expression in patient cells. The analysis of the breakpoints of the three deletions described in the study, showed that the deletions involved Alu elements, *C-rich* elements, MIR and low complexity repeats consisting of DNA transposons n(TA), indicating that the three deletions are located in repeated sequences prone to genomic rearrangements.

The first non-coding exon of XIAP was commonly removed in these three deletions, we showed that this region has a promoter activity, and by CRISPR-Cas9 genome editing in primary T cells we demonstrated that the non-coding exon1 contains key promoter sequences required for XIAP protein expression. Importantly, non-coding exons are not captured by WES and are often not included in targeted sequencing panels for different genetic diseases including those for primary immunodeficiencies (PIDs). We further analyzed 463 genes known to cause PIDs for the presence of non-coding exons. 42% (196 genes) of the genes harbors non-coding exons, and among them 79% (156 genes) are predicted to contain regulatory promoter elements based on ENCODE (representing a total of 40609bp) (**data not shown**). This is thus rather surprising that non-coding exons are still not well considered in the different genetic diagnostic

tools. Importantly, our results highlight and provide a clear demonstration that genetic variations in non-coding exons can lead to genetic disease and should be considered for sequencing when no genetic variations in coding regions are identified.

Our study also points out that protein expression analysis, that can be viewed as time consuming, remains one accurate way to achieve an unambiguous diagnosis, when in first intention genetic analysis fails.

Supplementary Information

The online version contains supplemental data that include supplemental material and methods, 6 supplemental figures and 3 tables.

Web resources

Online Medelian Inheritance in Man, <http://www.omim.org/>
ENCODE data in the UCSC Genome Browser, <https://genome.ucsc.edu/>
RepeatMasker program, software package: Smit A., (RepeatMasker Open, 2013-2015), <https://www.repeatmasker.org/faq.html/>
Bioinfo-fr, Human genome repeated elements, Devailly G., (Bioinfo-fr, 2017), <https://bioinfo-fr.net/>
Human Gene Mutation Database, HGMD 2020.4, Human Gene Mutation Database - Cardiff University, <http://www.hgmd.cf.ac.uk>

Funding

This work was supported by grants from the Ligue Contre le Cancer-Equipe Labélisée (France; to S. L.), Institut National de la Santé et de la Recherche Médicale (France), exome sequencing was funded by the Rare Diseases Foundation (France; to S.L.), the Agence Nationale de Recherche (ANR, France) (ANR-18-CE15-0025-01 to S.L. and ANR-10-IAHU-01 to Institut Imagine), the Société Française de Lutte contre les Cancers et Leucémies de l'Enfant et de l'Adolescent, AREMIG (France; to S.L.), and the Fédération Enfants et Santé (France ; to S.L.). S. L. is a senior scientist at the Centre National de la Recherche Scientifique (France). Z.S is supported by the Fondation ARC pour la recherche sur le Cancer France.

Conflict of interest/Competing interests

The authors declare no potential conflicts of interest.

Availability of data and material

All material and data are available on request

427 **Code availability**

428 All code are available on request

429 **Author's contributions**

430 Z.S., K.T. and C.B. designed, performed experiments and analyzed the data. K.T. A.H., F. J-H,
431 F.T., M.L.L., C.B. and C.L. performed experiments and analyzed the data. A.H., H.K., A.P.,
432 T.I., S.S, T.T. M.Y. identified the patients, provided clinical and analyzed the data. S.L. and
433 Z.S. wrote the manuscript. S. L. designed and supervised the research.

434 **Ethics approval**

435 The study and protocols conform to the 1975 Declaration of Helsinki as well as to local
436 legislation and ethical guidelines from the Comité de protection des personnes de l'Ile de France
437 II and the French advisory committee on data processing in medical research.

438 **Consent to participate**

439 Informed and written consent was obtained from donors, patients and families of patients.

440 **Consent for publication**

441 All authors consent for publication of the manuscript

442

References

1. Rigaud S, Fondaneche MC, Lambert N, Pasquier B, Mateo V, Soulas P, et al. XIAP deficiency in humans causes an X-linked lymphoproliferative syndrome. *Nature*. 2006;444(7115):110-4.
2. Worthey EA, Mayer AN, Syverson GD, Helbling D, Bonacci BB, Decker B, et al. Making a definitive diagnosis: successful clinical application of whole exome sequencing in a child with intractable inflammatory bowel disease. *Genet Med*. 2011;13(3):255-62.
3. Speckmann C, Ehl S. XIAP deficiency is a mendelian cause of late-onset IBD. *Gut*. 2014;63(6):1031-2.
4. Aguilar C, Lenoir C, Lambert N, Begue B, Brousse N, Canioni D, et al. Characterization of Crohn disease in X-linked inhibitor of apoptosis-deficient male patients and female symptomatic carriers. *J Allergy Clin Immunol*. 2014;134(5):1131-41 e9.
5. Ono S, Okano T, Hoshino A, Yanagimachi M, Hamamoto K, Nakazawa Y, et al. Hematopoietic Stem Cell Transplantation for XIAP Deficiency in Japan. *J Clin Immunol*. 2017;37(1):85-91.
6. Chen RY, Li XZ, Lin Q, Zhu Y, Shen YY, Xu QY, et al. Epstein-Barr virus-related hemophagocytic lymphohistiocytosis complicated with coronary artery dilation and acute renal injury in a boy with a novel X-linked inhibitor of apoptosis protein (XIAP) variant: a case report. *BMC Pediatr*. 2020;20(1):456.
7. Yang X, Hoshino A, Taga T, Kunitsu T, Ikeda Y, Yasumi T, et al. A female patient with incomplete hemophagocytic lymphohistiocytosis caused by a heterozygous XIAP mutation associated with non-random X-chromosome inactivation skewed towards the wild-type XIAP allele. *J Clin Immunol*. 2015;35(3):244-8.
8. Eckelman BP, Salvesen GS, Scott FL. Human inhibitor of apoptosis proteins: why XIAP is the black sheep of the family. *EMBO Rep*. 2006;7(10):988-94.
9. Yabal M, Muller N, Adler H, Knies N, Gross CJ, Damgaard RB, et al. XIAP restricts TNF- and RIP3-dependent cell death and inflammasome activation. *Cell Rep*. 2014;7(6):1796-808.
10. Krieg A, Correa RG, Garrison JB, Le Negrato G, Welsh K, Huang Z, et al. XIAP mediates NOD signaling via interaction with RIP2. *Proc Natl Acad Sci U S A*. 2009;106(34):14524-9.
11. Parackova Z, Milota T, Vrabcova P, Smetanova J, Svaton M, Freiburger T, et al. Novel XIAP mutation causing enhanced spontaneous apoptosis and disturbed NOD2 signalling in a patient with atypical adult-onset Crohn's disease. *Cell Death Dis*. 2020;11(6):430.
12. Damgaard RB, Nachbur U, Yabal M, Wong WW, Fiil BK, Kastirr M, et al. The ubiquitin ligase XIAP recruits LUBAC for NOD2 signaling in inflammation and innate immunity. *Mol Cell*. 2012;46(6):746-58.
13. Damgaard RB, Fiil BK, Speckmann C, Yabal M, zur Stadt U, Bekker-Jensen S, et al. Disease-causing mutations in the XIAP BIR2 domain impair NOD2-dependent immune signalling. *EMBO Mol Med*. 2013;5(8):1278-95.
14. Marsh RA, Madden L, Kitchen BJ, Mody R, McClimon B, Jordan MB, et al. XIAP deficiency: a unique primary immunodeficiency best classified as X-linked familial hemophagocytic lymphohistiocytosis and not as X-linked lymphoproliferative disease. *Blood*. 2010;116(7):1079-82.
15. Filipovich AH, Zhang K, Snow AL, Marsh RA. X-linked lymphoproliferative syndromes: brothers or distant cousins? *Blood*. 2010;116(18):3398-408.
16. Zeissig Y, Petersen BS, Milutinovic S, Bosse E, Mayr G, Peuker K, et al. XIAP variants in male Crohn's disease. *Gut*. 2015;64(1):66-76.

17. Latour S, Aguilar C. XIAP deficiency syndrome in humans. *Semin Cell Dev Biol.* 2015;39:115-23.
18. Davidson AE, Liskova P, Evans CJ, Dudakova L, Noskova L, Pontikos N, et al. Autosomal-Dominant Corneal Endothelial Dystrophies CHED1 and PPCD1 Are Allelic Disorders Caused by Non-coding Mutations in the Promoter of OVOL2. *Am J Hum Genet.* 2016;98(1):75-89.
19. Wakabayashi A, Ulirsch JC, Ludwig LS, Fiorini C, Yasuda M, Choudhuri A, et al. Insight into GATA1 transcriptional activity through interrogation of cis elements disrupted in human erythroid disorders. *Proc Natl Acad Sci U S A.* 2016;113(16):4434-9.
20. Thaventhiran JED, Lango Allen H, Burren OS, Rae W, Greene D, Staples E, et al. Whole-genome sequencing of a sporadic primary immunodeficiency cohort. *Nature.* 2020;583(7814):90-5.
21. Turro E, Astle WJ, Megy K, Graf S, Greene D, Shamardina O, et al. Whole-genome sequencing of patients with rare diseases in a national health system. *Nature.* 2020;583(7814):96-102.
22. Li J, Woods SL, Healey S, Beesley J, Chen X, Lee JS, et al. Point Mutations in Exon 1B of APC Reveal Gastric Adenocarcinoma and Proximal Polyposis of the Stomach as a Familial Adenomatous Polyposis Variant. *Am J Hum Genet.* 2016;98(5):830-42.
23. Horn S, Figl A, Rachakonda PS, Fischer C, Sucker A, Gast A, et al. TERT promoter mutations in familial and sporadic melanoma. *Science.* 2013;339(6122):959-61.
24. French JD, Edwards SL. The Role of Noncoding Variants in Heritable Disease. *Trends Genet.* 2020;36(11):880-91.
25. Gerstein MB, Kundaje A, Hariharan M, Landt SG, Yan KK, Cheng C, et al. Architecture of the human regulatory network derived from ENCODE data. *Nature.* 2012;489(7414):91-100.
26. Martin E, Palmic N, Sanquer S, Lenoir C, Hauck F, Mongellaz C, et al. CTP synthase 1 deficiency in humans reveals its central role in lymphocyte proliferation. *Nature.* 2014;510(7504):288-92.
27. Benyelles M, Episkopou H, O'Donohue MF, Kermasson L, Frange P, Poulain F, et al. Impaired telomere integrity and rRNA biogenesis in PARN-deficient patients and knock-out models. *EMBO Mol Med.* 2019;11(7):e10201.
28. Venot Q, Blanc T, Rabia SH, Berteloot L, Ladraa S, Duong JP, et al. Targeted therapy in patients with PIK3CA-related overgrowth syndrome. *Nature.* 2018;558(7711):540-6.
29. Rosain J, Oleaga-Quintas C, Deswarte C, Verdin H, Marot S, Syridou G, et al. A Variety of Alu-Mediated Copy Number Variations Can Underlie IL-12Rbeta1 Deficiency. *J Clin Immunol.* 2018;38(5):617-27.
30. Simonetti L, Bruque CD, Fernandez CS, Benavides-Mori B, Delea M, Kolomenski JE, et al. CYP21A2 mutation update: Comprehensive analysis of databases and published genetic variants. *Hum Mutat.* 2018;39(1):5-22.
31. Li H, Durbin R. Fast and accurate long-read alignment with Burrows-Wheeler transform. *Bioinformatics.* 2010;26(5):589-95.
32. Consortium EP, Birney E, Stamatoyannopoulos JA, Dutta A, Guigo R, Gingeras TR, et al. Identification and analysis of functional elements in 1% of the human genome by the ENCODE pilot project. *Nature.* 2007;447(7146):799-816.
33. Menoret S, De Cian A, Tesson L, Remy S, Usal C, Boule JB, et al. Homology-directed repair in rodent zygotes using Cas9 and TALEN engineered proteins. *Sci Rep.* 2015;5:14410.
34. Concordet JP, Haeussler M. CRISPOR: intuitive guide selection for CRISPR/Cas9 genome editing experiments and screens. *Nucleic Acids Res.* 2018;46(W1):W242-W5.

35. Aguilar C, Latour S. X-linked inhibitor of apoptosis protein deficiency: more than an X-linked lymphoproliferative syndrome. *J Clin Immunol*. 2015;35(4):331-8.
36. van Zelm MC, Geertsema C, Nieuwenhuis N, de Ridder D, Conley ME, Schiff C, et al. Gross deletions involving IGHM, BTK, or Artemis: a model for genomic lesions mediated by transposable elements. *Am J Hum Genet*. 2008;82(2):320-32.
37. Verdin H, D'Haene B, Beysen D, Novikova Y, Menten B, Sante T, et al. Microhomology-mediated mechanisms underlie non-recurrent disease-causing microdeletions of the FOXL2 gene or its regulatory domain. *PLoS Genet*. 2013;9(3):e1003358.
38. Casper J, Zweig AS, Villarreal C, Tyner C, Speir ML, Rosenbloom KR, et al. The UCSC Genome Browser database: 2018 update. *Nucleic Acids Res*. 2018;46(D1):D762-D9.

Table 1. Clinical presentation and data of patients.

	Patient 1	Patient 2	Patient 3
Age at initial presentation	1 m. o.	1 y. 6 m. o.	1 y. o. HLH ; 9 y.o. colitis
Current age	9 y.	5 y.	21 y.
Origin	South American (Argentina)	Asian (Japan)	Asian (Japan)
Family history	-	-	-
HLH	+	+	+
Recurrent HLH	+	+	+
Fever	+	-	-
Splenomegaly	+ (persistent, never resolved)	-	-
Cytopenia	+	+	-
Thrombocytopenia	+	+	-
EBV	+	-	-
Other infections	Rotavirus diarrhea and UTI by K. pneumoniae at 2 m. o. ; CMV reactivation during admission for HLH at 2 y. o. ; 1 episode of pneumonia at 5 y. o. (treated with amoxicillin-clavulanate)	-	-
Hypogammaglobunemia	-	-	-
Inflammatory bowel disease/colitis	-	-	+
Treatments	Methylprednisolone, + anti-thymocyte globulin (for HLH) ; Rituximab (for HLH) ; maintenance therapy with cyclosporine and SCIG	Dexamethasone (for HLH)	Methylprednisolone (for HLH), Prednisolone, Infliximab, Tacrolimus, Adalimumab (for colitis)
Allogeneic HSCT	+	-	+
Surgery	-	-	Hemicolectomy, Total colectomy, Ileostomy

556 Abbreviations : HLH, hemophagocytic lymphohistiocytosis ; ND, no data ; EBV, Epstein-Barr virus ; HSCT,
557 hematopoietic stem cell transplantation ; SCIG, Subcutaneous immunoglobulin ; UTI, urinary tract infection ; CMV,
558 cytomegalovirus ; y., year(s) ; m., month(s) ; o., old ; + yes or positive, - no or negative.
559

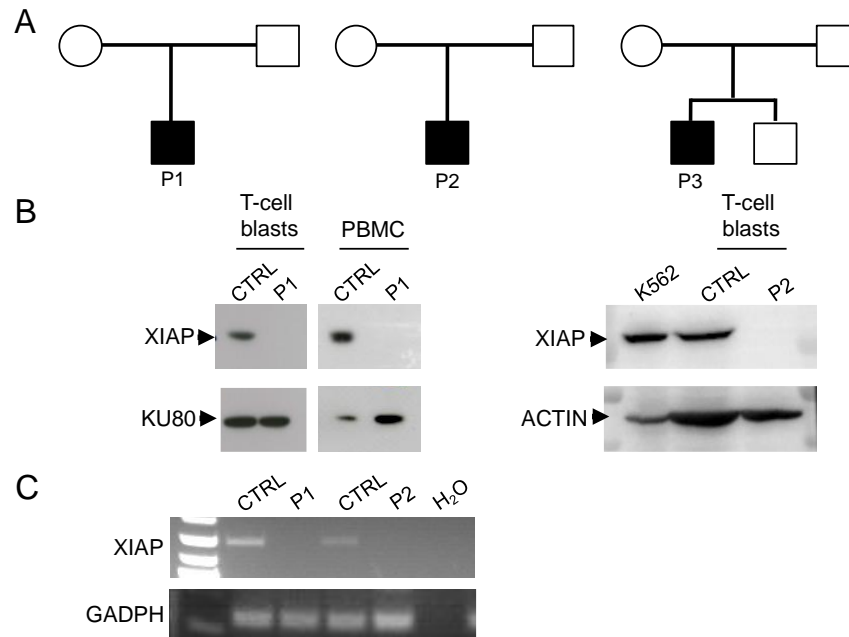


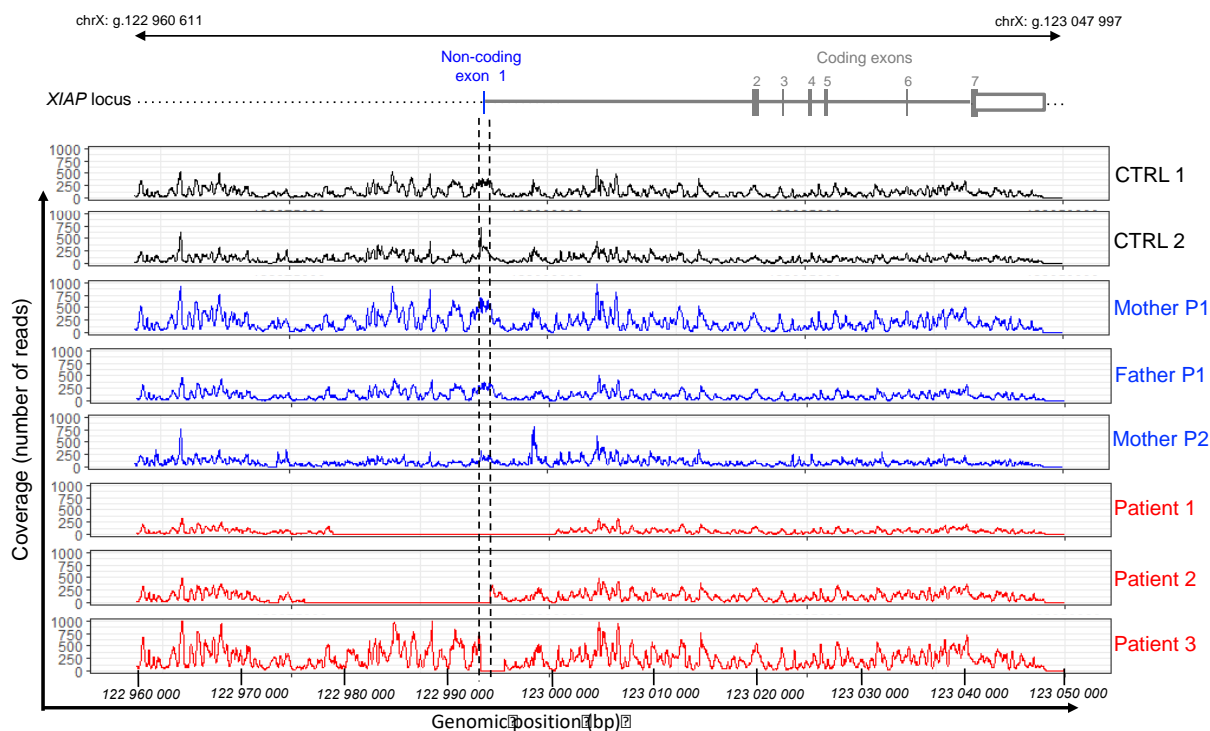
Figure 1. Defective XIAP expression in three patients with clinical-like features of XIAP deficiency.

(A) Pedigrees of the three unrelated families presenting XLP-2-like features. Black boxes represent affected individuals. An identification number assigned to each patient is indicated (P1, P2 and P3).

(B) Expression of XIAP protein by western blot in T-cell blasts and PBMCs from a healthy control (CTRL) and P1 (left panels); in the K562 cell line and T-cell blasts from a healthy control (CTRL) and the P2 (right panels). Blots of KU80 and ACTIN as loading controls.

(C) Expression of *XIAP* transcripts by PCR in T-cell blasts from CTRL, P1 and P2. GAPDH was measured in the same samples as a loading control for PCR.

571



572

573

574

575

576

577

578

579

580

581

582

583

584

585

Figure 2. Identification of large deletions encompassing the non-coding first exon of XIAP in 3 patients with XIAP deficiency-like features.

Sequencing coverage obtained by NGS of the XIAP locus (g.122960611 to g.123047997) of the three patients (Patient 1, Patient 2, and Patient 3), both parents of patient 1 (Father P1 and Mother P1), mother of patient 2 (Mother P2) and two healthy controls (CTRL 1 and CTRL 2). Vertical pale gray lines highlight the position of the exons. Red shading indicates deletions. Vertical dashed lines indicate the common deleted region in the 3 patients encompassing the non-coding exon1. The XIAP locus and the XIAP gene structure is depicted on the top with coding exons (grey boxes) and the first non-coding exon (blue box) joined by introns (grey lines). Genomic positions from GRCh37-hg19 human genome assembly.



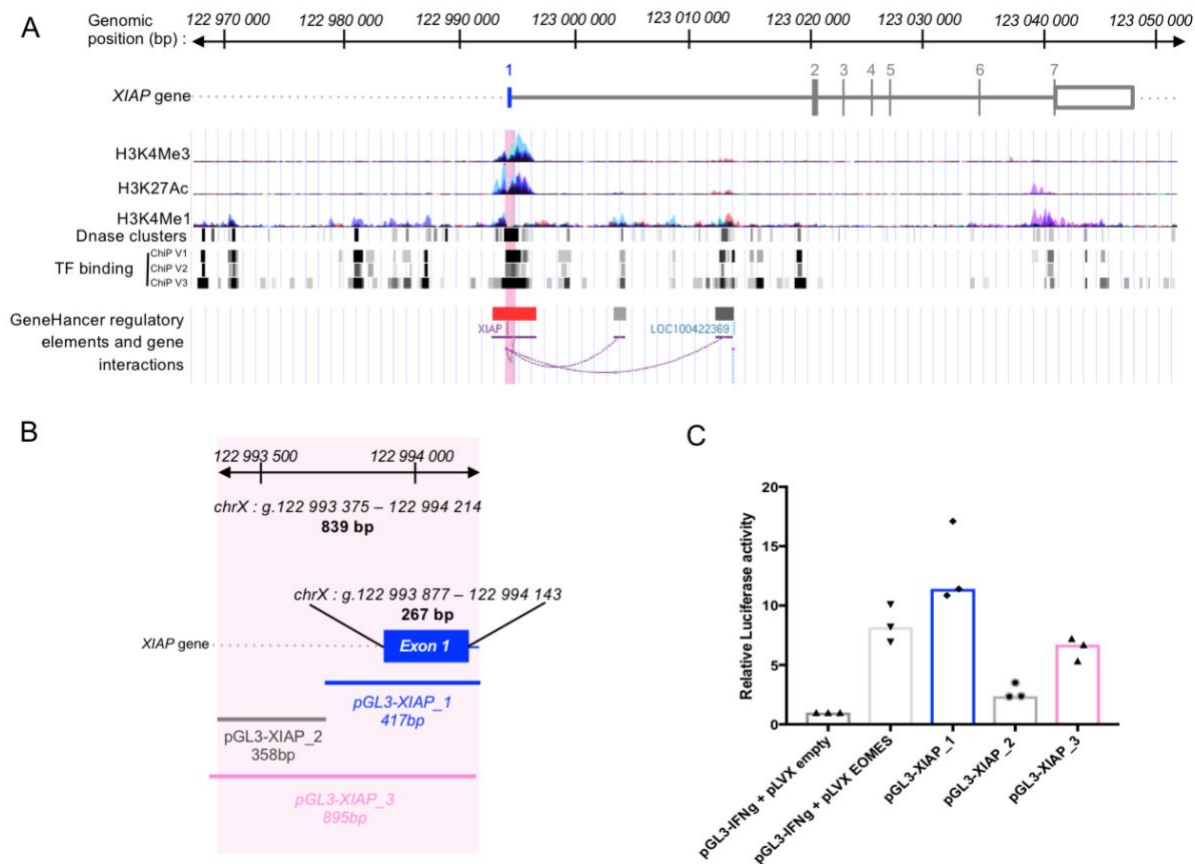


Figure 4. The common deleted region in the three patients is an active promoter sequence.

(A) Analysis of the common deleted region in the three patients containing the first non-coding exon of *XIAP* for regulatory elements and chromatin modifications from UCSC genome browser of the ENCODE project. Histone modifications H3K4Me3, (indicative of promoters), H3K27Ac (indicative of active enhancers) and H3K4Me1 (indicative of regulatory regions) from seven different cell lines are shown in this track. Each cell line is represented by a particular color. DNA clusters corresponding to DNaseI hypersensitivity (indicative of open chromatin) and binding of transcription factors (TF) from different ChIP data bases are shown by gray and black boxes/vertical lines that indicates a hypersensitive region or a peak cluster of transcription factor occupancy. The darkness is proportional to the maximum signal strength observed in different cell lines tested. GeneHancer Regulatory Elements indicative of elements with enhancers (in gray) and promoters (in red), and their inferred target genes connected by curves are indicated at the bottom of the panel. Gray and black boxes correspond to weak and strong enhancer regions, respectively. The gene structure of *XIAP* is depicted on the top with genome scale of the *XIAP* locus (as shown in **Figure 2**) from hg19 human genome assembly. The common deleted region is highlighted by a large pink vertical line.

(B) Schematic representation of the commonly deleted region of 839bp sub-divided in two regions of 417bp (containing the non-coding exon1) and 359bp containing the flanking 5' sequences that were tested in the pGL3-basic (firefly luciferase) vector.

(C) Relative dual luciferase activity data from HEK293 cells co-transfected with pRL-CMV (green *Renilla* luciferase) and pGL3-basic (red firefly luciferase) with a 895bp fragment containing the 839bp deleted region (pGL3-XIAP_3), the 417bp (pGL3-XIAP_1) or the 358bp pGL3-XIAP_2 sequences as depicted in (B). Positive control activity corresponds to EOMES-induced activity of the proximal IFN γ promoter. Negative control activity corresponding to the basal activity of the proximal IFN γ promoter (without EOMES) was normalized to 1, and the relative luciferase activity of all the sequences was expressed with respect to this normalized negative control. Data from three independent experiments.

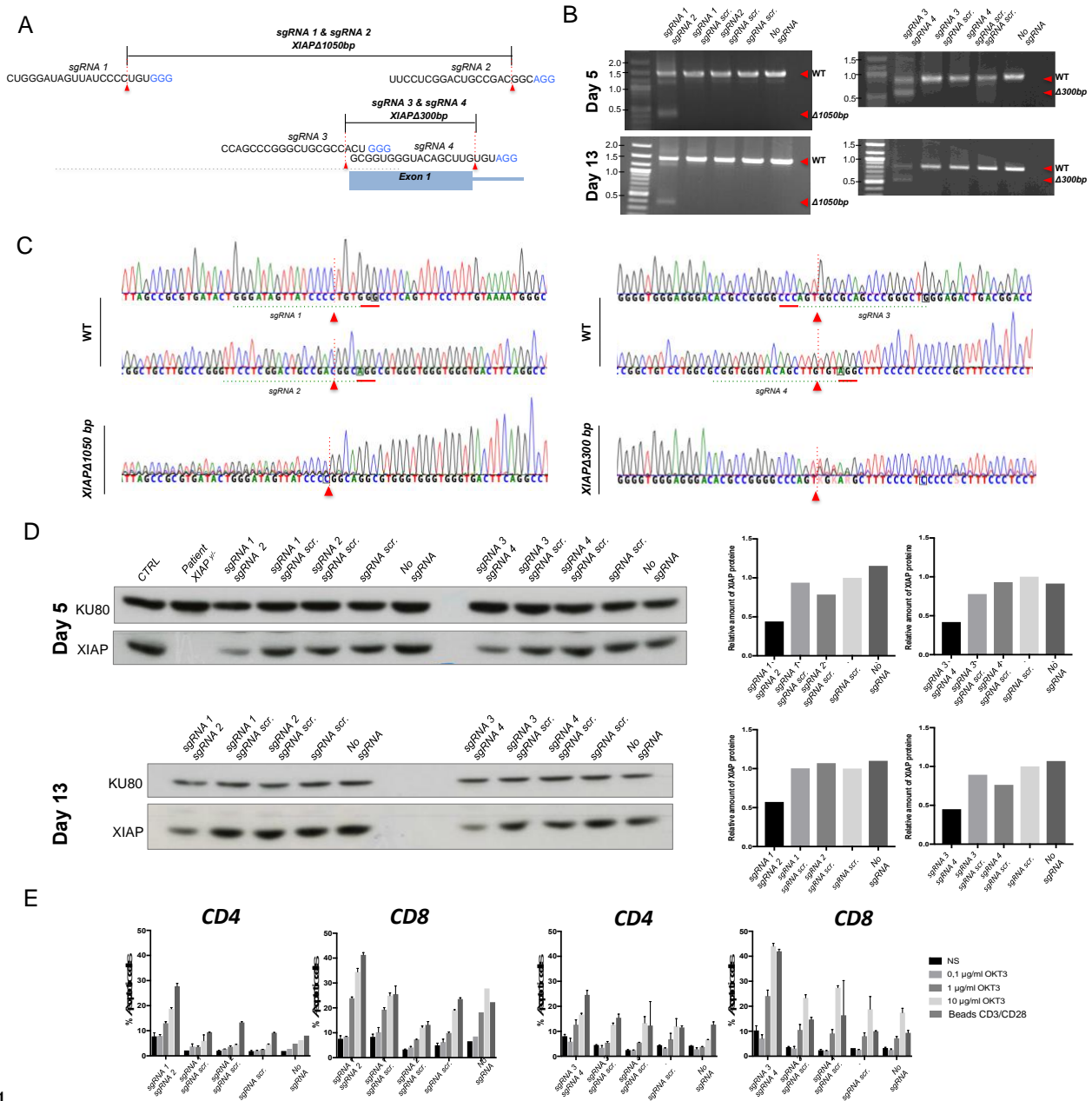


Figure 5. Dual-targeting by CRISPR-Cas9 to excise the XIAP non-coding exon1 in primary T cells leads to the decrease of XIAP protein expression. (A) Schematic representation of CRISPR-Cas9-mediated deletions of 105bp (*XIAP*Δ1050bp) and 300bp (*XIAP*Δ300bp) encompassing the 839bp region (shaded in pink) and the non-coding exon1 (blue box) respectively. The sequences of sgRNAs (sgRNA1, sgRNA2, sgRNA3 and sgRNA4) are indicated with the PAMs in blue and cleavage sites highlighted with red arrow. (B) PCR analysis over the target sites in *XIAP* at two time points (day 5 and day 13 after transfection) of genomic DNA of primary T cells transfected with the CAS9 and both sgRNA1 and sgRNA2 (sgRNA1/sgRNA2) (left panels), sgRNA3 and sgRNA4 (sgRNA3/sgRNA4) (right panels) or each single sgRNA in the presence of a scramble sgRNA (sgRNA scr.) or without sgRNA (no sgRNA). Wild-type (WT) and *XIAP*Δ1050bp amplicons (left panels) for sgRNA1/sgRNA2 are expected at 1453bp and 403bp respectively, while the WT amplicon and *XIAP*Δ300bp (right panels) for sgRNA3/sgRNA4 are expected at 843 bp and 543 bp respectively. WT, *XIAP*Δ300bp and *XIAP*Δ1050bp are depicted by red arrows on the right. (C) Chromatograms from Sanger sequencing of PCR products of panel B showing the wild-type, the *XIAP*Δ1050bp and the *XIAP*Δ300bp sequences. Breakpoints shown by red arrows. (D) Western blots (on the left) of lysates from primary T cells of panel B. A lysate from XIAP-deficient patient (Patient XIAP^Δ) was analyzed as a negative control. Blots of KU80 as loading controls. Graphs (on the right) from densitometry quantifications of XIAP expression normalized to KU80 western blots. (E) Activation-induced cell death of primary T cells of panel B, in response to anti-CD3 stimulation with OKT3 at different concentrations or anti-CD3/CD28-coated beads.